Lasers in Surgery and Medicine 18:301–308 (1996)

Photosensitization of the Rat Endometrium Following 5-Aminolevulinic Acid Induced Photodynamic Therapy

Rolf A. Steiner, MD, Yona Tadir, MD, Bruce J. Tromberg, PhD, Tatiana Krasieva, PhD, Armen T. Ghazains, Pius Wyss, MD, and Michael W. Berns, PhD

Beckman Laser Institute and Medical Clinic (R.A.S., Y.T., B.J.T., T.K., A.T.G., P.W., M.W.B.) and Department of Obstetrics and Gynecology (Y.T.), University of California, Irvine, Irvine, California 92715; Department of Obstetrics and Gynecology, University Hospital of Zurich, Zurich, CH 8091 Switzerland (R.A.S., P.W.)

Background and Objective: **The impact of photodynamic therapy (PDT) on the endometrium following topical application of 5-aminolevulinic acid (ALA) was studied in a rat model.** ***Study Design/ Materials and Methods:*** **Fluorescence microscopy revealed peak ALA to protoporphyrin IX (Pp IX) conversion 3–6 hours after application. Significantly higher Pp IX levels were observed in the endometrial glands compared with endometrial stroma and myometrium.**
Results: **Histological studies showed PDT-induced endometrial destruction with atrophy 7–10 weeks after treatment. Reproductive performance studies demonstrated significant implantation failure in the treated uterine horns compared with controls. The number of implantation sacs in the treated and untreated horns was 0.4 ± 0.3 and 8.9 ± 1.0, respectively ($P < 0.01$).**
Conclusion: **We conclude that the high rate of Pp IX conversion in the endometrial glands can be exploited to treat dysfunctional uterine bleeding with PDT. In addition, this concept may also be applied to study endometrial regeneration and embryo implantation mechanisms.**

Key words: 5-aminolevulinic acid, implantation, photodynamic therapy, reproductive performance

INTRODUCTION

Photodynamic therapy (PDT) refers to the light activation of a photosensitizer to generate highly reactive oxygen intermediates [1–3]. These intermediates irreversibly oxidize essential cellular components, causing local injury and necrosis [4–6]. The human endometrium exhibits several features that satisfy requirements for effective PDT: (1) It is easily accessible, (2) it is only a few millimeters thick, and (3) it is surrounded by a thick myometrium, which acts as a protective light barrier for intraabdominal organs. Moreover, it is a vascular tissue that proliferates rapidly following hormonal stimulation. The substantial effect PDT has on tumor microvasculature [7–9] suggests that it should be highly effective in the well-vascularized endometrium.

Promising results have been reported by several authors who investigated PDT for surgically induced endometriosis [10] and for selective endometrial ablation in experimental animals [11]. A major drawback of PDT as a treatment modality is the persistent skin photosensitivity that lasts 4–6 weeks following systemic administration of some photosensitizers [12–14]. Based upon our previous results on the uptake and distribution of Photofrin® in the rat uterus [15], our goal was to

Accepted for publication January 31, 1995.

Reprint requests to Y. Tadir, M.D., Professor, Obstetrics and Gynecology, Beckman Laser Institute and Medical Clinic, University of California, Irvine, 1002 Health Science Rd., Irvine, CA 92715.

Dr. Berns did not participate in the editorial review of this article.

study the impact of PDT on the endometrium after local intrauterine application of a photosensitizer and laser light.

In this study we have analyzed the pharmacokinetic behavior of topically administered 5-aminolevulinic acid (ALA) and the morphologic characteristics of ALA-induced PDT in a rat animal model. 5-Aminolevulinic acid is a precursor of protoporphyrin IX (Pp IX) in the heme biosynthetic pathway. Heme biosynthesis is essential to life and takes place in all aerobic cells. The slowest process in heme synthesis is the step of converting Pp IX to heme. Therefore, the administration of exogenous ALA induces the accumulation of Pp IX, a strong photosensitizer [16,17]. Since cells vary in their capacity to generate Pp IX, ALA can provide an element of selectivity to PDT. We have evaluated cellular specificity by monitoring the spatial distribution of Pp IX in frozen uterine sections. Endometrial damage was measured by evaluating reproductive performance in PDT treated rats.

MATERIALS AND METHODS

Eighty-seven mature female Sprague-Dawley rats, weighing 275–320 g, were placed in a control setting of 12 hours darkness followed by 12 hours light for several days with free access to food and water. The estrous cycle was monitored by obtaining frequent vaginal smears in order to synchronize the treatment and fluorescence evaluation to the day of diestrous [18]. The choice of treatment and fluorescence evaluation was synchronized to the day of diestrous because this is the day in the cycle that is most independent of hormonal stimulation. The animals were divided into three groups for three complimentary studies: (1) determination of the uptake, distribution, and clearance of 5-aminolevulinic acid (Deprenyl USA Inc., Parsippany, NJ) in uterine layers following topical application by fluorescence microscopy; (2) morphological changes following intrauterine drug and light application (PDT); and (3) reproductive performance following PDT.

Fluorescence Study

Thirty-two animals were topically administered 15 mg ALA (58 mg/kg) on each uterine horn (white crystallized substance stored in dark at 4°C and dissolved in 0.15 ml sterile water shortly prior to injection). This dose is similar to that used by Yang et al. [19], who tested various doses (5–16 mg per uterine horn). The animals were anesthetized with ketamine (87 mg/kg) and xylazine (13 mg/kg) intramuscularly, and intrauterine injections were performed through a small incision in the abdominal wall, placing the ALA into the two uterine horns via a 1 ml tuberculin syringe with a 25G5/8 needle. The abdomen was closed with silk 3-0 suture, and all rats were allowed to recover from anesthesia in a darkened cage. The animals were sacrificed at 0.5, 1, 1.5, 2, 3, 6, 12, and 24 hours after drug administration using CO_2 asphyxiation. Data were obtained from four animals at each time point. Four rats receiving no drug were assigned as controls to determine background noise and autofluorescence levels. Shortly after sacrifice, six uterine specimens of 3–4 mm each were retrieved and placed in molds containing embedding medium for frozen sections (OCT media, Miles, Elkhart, IN). The blocks were rapidly frozen on dry ice and stored at −70°C in the dark.

Tissues were sectioned in low, diffuse light (Cryostat microtome, AO Reichert, Buffalo, NY) in 6 μm thick slices. Low-light level tissue fluorescence imaging was performed with a slow-scan, thermoelectrically cooled CCD camera system (model 57–180, Princeton Instruments, Trenton, NJ) with 16-bit-per-pixel dynamic range. A Zeiss Axiovert 10 inverted microscope was used (Zeiss, Oberkochen, Germany) with a 10× objective Zeiss Plan-NEOFLUAR (N.A. = 0.3) to visualize bright field and fluorescence images of the tissue frozen sections. A 100W mercury lamp filtered through a 405 nm bandpass filter provided the excitation light that was reflected onto the sample through a dichroic mirror (Zeiss FT 420, Oberkochen, Germany). Emission light was isolated with a 635 nm broad bandpass filter.

Instrument control and image acquisition were performed with a MacIntosh IIfx computer coupled to the camera via an IEEE-488 interface (National Instruments Inc., Austin, TX). IPlab software (Signal Analytics Corp., Vienna, VA) was used to process images and to manage all camera operations. Sample photodegradation was minimized in bright field and fluorescence, respectively, by (1) locating the region of interest under low, orange/red light illumination and (2) limiting the arc-lamp exposure to 1–2 seconds by electronically synchronizing the camera and lamp shutters. In order to estimate light distribution, background images were acquired from blank slides under conditions identical to sample measurements. Dark noise levels were determined by acquiring images without source illumination. All fluorescence images were normalized by the

following algorithm in order to correct for dark noise and non-uniform illumination:

$$\text{Normalized fluorescence image} = \frac{\text{mean (background} - \text{dark noise)}}{\text{image (background} - \text{dark noise)}} \times \text{image (fluorescence} - \text{dark noise)},$$

where mean (background − dark noise) is the mean gray-scale value for the dark-noise–corrected background image. Cross-sectional images of the rat uterus were divided into three structurally distinct layers for comparative analysis: (1) endometrial glands, (2) endometrial stroma, and (3) myometrium.

Histology Study

Twenty-four rats were photosensitized as described earlier. Three hours after drug administration, the animals were re-anesthetized and the left uterine horn was carefully exposed. A few millimeters distal to the uterine bifurcation, the uterine wall was punctured with a 20 G needle. A 400 μm fiber with a 2.0 cm long cylindrical diffusing tip and a diameter of .8 mm (PDT Systems, Buellton, CA) was inserted into the cavity through the perforation site. Then 133 mW of red light at 630 nm was released into the fiber over 13 minutes and 20 seconds. This corresponds to a 212 J/cm^2 incident optical dose at the surface of the applicator. The uterine horns were moistened with saline during the procedure to prevent drying and serosal damage. At the end of the laser treatment, the abdomen was closed with one layer of Dexon 4-0 suture and the skin was secured with staples. Recovery was monitored until return to normal activity. The rats were housed individually with free access to food and water. At 24 and 48 hours, and at 4, 7, 14, and 21 days after PDT, four rats were sacrificed at each time point as in group A. Six control rats received 80 J/cm^2 of light without drug and were sacrificed on days 2, 4, and 7.

The excised genital tract was retrieved and fixed in 10% neutral buffered formalin after photodocumentation. Cylindrical samples were taken from the treated area of the left horn and from the control side, and were further processed for hematoxylin and eosin staining. Sections (4–6 μm) were microscopically examined and documented.

Reproductive Performance

Nine rats were treated as described in the previous section. Three to 4 weeks following PDT of the left uterine horn, the animals were mated with mature male Sprague-Dawley rats. The females were sacrificed in the second trimester of pregnancy as described. The location and number of implantation sacs in the treated uterine horn and the control side were noted and photographed. Specimens of the treated uterine horns were also retrieved for histologic studies. Control groups consisted of six animals treated with the same amount of topical ALA without illumination and another six rats with the same illumination used for PDT but without drug priming.

Skin photosensitivity. All animals were also light treated in a shaved skin area at the upper right quadrant of the abdomen with a light dose of 100 J/cm^2 and a spot size of 1 cm^2 (160 mW over 8 minutes and 20 seconds at a power density of 200 mW/cm^2). The treated skin area was checked immediately after light application and during recovery at 1 hour intervals, and then daily until the animals were sacrificed.

Light delivery system. An argon-pumped dye laser operating at 630 nm (argon laser model 171, and dye laser model 375, Spectra Physics, Mountain View, CA) was transmitted through the 400 μm fiber with a 2 cm cylindrical diffusing tip. A Clinical Hartridge Reversion spectroscope (Ealing Electro-Optics, South Natick, MA) was used to verify the accuracy of the laser wavelength to ±1 nm. By using a fiber splitter (model 1220, Laser Therapeutics, Inc., Buellton, CA) connected to the laser source by a 200 μm core fiber (model 52120-A05, PDT Systems, Buellton, CA), two to three animals could be light treated simultaneously.

For irradiation of the skin, the laser beam was coupled into a 400 μm fused-silica fiber optic using a Spectra-Physics (Mountain View, CA) model 316 fiber optic coupler. The output end of the fiber terminated at a microlens that focused the laser radiation into a circular field of uniform light intensity with a spot size of 1 cm. Laser irradiation emanating from the diffusing fiber tip and the microlens, respectively, was monitored with a power meter (model 210, Coherent Corp., Palo Alto, CA) before and after treatment.

Temperature measurements. In order to demonstrate the dynamics of temperature changes during PDT, the surface temperature of the treated uterine horn was measured in two rats before, during, and after photodynamic treatment. An infrared thermal camera (model 600, Inframetrics, Bedford, MA) was used to scan the field of view horizontally and vertically, and to

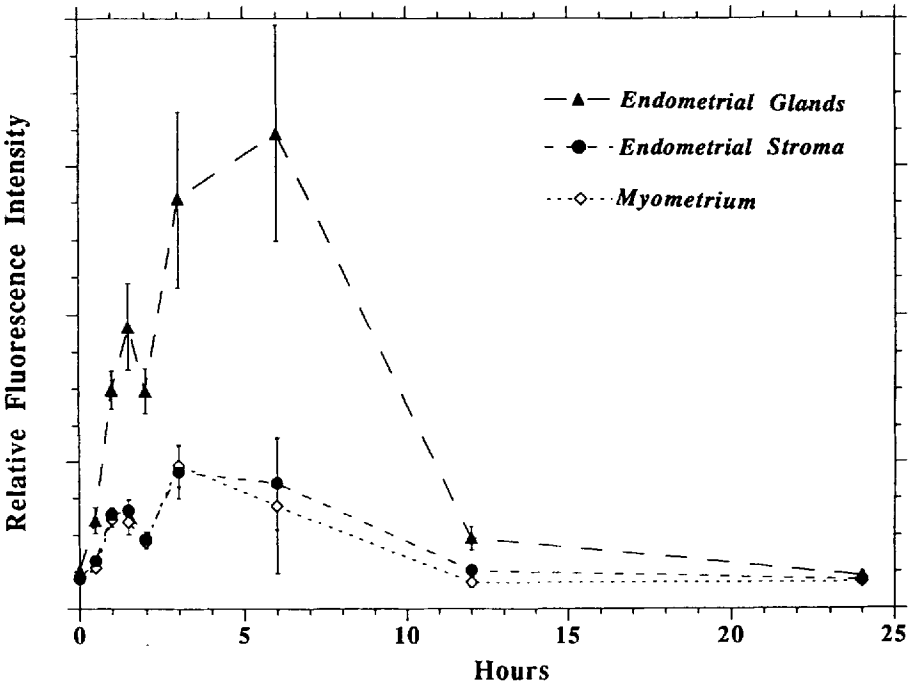

Fig. 1. Kinetic curve of the fluorescence (means with standard error) in the uterine tissue after intrauterine injection of ALA (58 mg/kg in .15 ml sterile H_2O).

produce images at a rate of 30 frames per second. The thermal camera employs a mercury-cadmium-telluride (Hg Cd Te) detector that is sensitive over 8–12 μm and can detect changes of 0.1°C.

Statistical Analysis

The reproductive performance outcome between the treated area of the left uterine horn and the corresponding area of the control horn was analyzed with the paired two-tail Student *t*-test and the paired Wilcoxon signed rank test. Significance was considered at $P < 0.05$. Cited results refer to the Wilcoxon signed rank test. All data are presented as mean ± SE.

RESULTS

Fluorescence Study

Analysis of digital fluorescence microscopy following the topical application of ALA revealed peak values at 3–6 hours with significantly higher concentrations in the endometrial glands (Fig. 1). There was a gradual decrease at 6–12 hours and relative fluorescence values in all layers eventually converge and gradually return to pre-injection levels at 24 hours. A cross section of rat uteri at 3 hours following topical application of ALA is illustrated in Figure 2. The two images represent the same specimen: (a) a bright field image of the frozen section in which the endometrium (glands and stroma) and the myometrium (inner layer, circular; outer layer, longitudinal) are clearly visible; (b) fluorescence micrograph of the same image in which the endometrial glands contain relatively higher fluorescence. The endometrial stroma and myometrium are diffusely distributed with fluorescing cells. As shown in the image, fluorescence in all tissue levels is relatively high, but glandular fluorescence is predominant (Fig. 1).

The mean thickness of the rat endometrium was .78 mm ± 0.06 mm. High magnification of endometrial glands (Fig. 3) revealed that the fluorescing protoporphyrin IX is located in the cytoplasm and the membranes of cylindrical epithelial cells but not in the nucleus.

Morphologic Study

Significant macroscopic changes were noted following PDT. Immediately after termination of light application, blanching of the treated area of the uterine horn was observed. Blanching gradually decreased up to the fourth day. During this period there was a tendency toward myometrial contraction, suggesting a higher functional sensi-

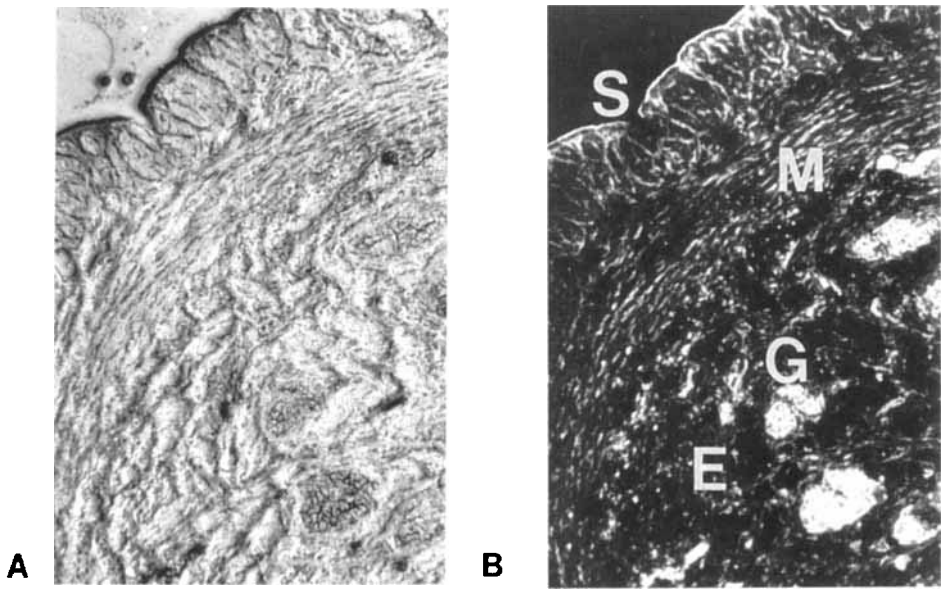

Fig. 2. Bright field image (**A**) and fluorescence micrograph (**B**) of the rat uterus 3 hours following topical application of ALA (58 mg/kg in .15 ml sterile H_2O intrauterine). Note the high fluorescence in the endometrial glands as compared with the myometrium, suggestive of potential selective destruction by PDT. E = endometrium; G = gland; M = myometrium; S = stroma.

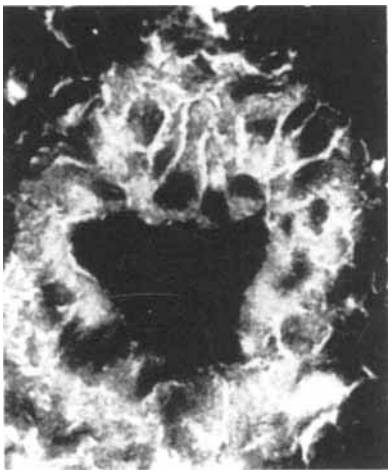

Fig. 3. Cross section of an endometrial gland (high power magnification, 100×) after topical application of ALA (58 mg/kg in .15 ml sterile H_2O intrauterine). The nucleus of the epithelial cells has no fluorescence.

tivity of the myometrium. Edematous thickening and rigidity of the uterine horn increased up to the fourth day after treatment. These signs diminished thereafter, and at 2–3 weeks post-PDT the diameter of the left uterine horn gradually decreased in the treated area. Long-term follow-up of the treated horns (7–10 weeks) revealed atrophy and thinning, as is described in the reproductive performance study.

Microscopic changes. Twenty-four hours following PDT the left uterine horns showed necrosis of the epithelial cells lining the lumen and the tissue in the lamina propria. Fibrinous debris were often found in the lumen. The endometrial glands appeared in various stages of disintegration, which ranged from early degenerative change to complete liquification with only the glandular outlines remaining visible. In some animals the tunica muscularis was also affected, with lesions ranging from vacuolar degeneration to edema of the interstitial tissue, and to complete necrosis of the muscle cells. Forty-eight hours after treatment there were areas of progressed necrosis (compared with those observed at 24 hours) and signs of early epithelial regeneration. Vascular collapse with some fibrinous debris of either embolus or thrombi was present in areas of severe tissue necrosis.

Complete regeneration of the cylindric epithelium lining the lumen and some regeneration of the endometrial glands was present 7 days after PDT. In this regenerative stage, many arteries presented with a complete endothelial lining, although necrotic debris still persisted beneath the endothelium. The regeneration process continued

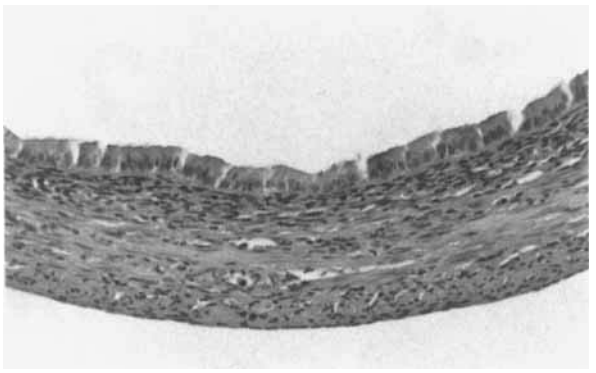

Fig. 4. Cross section of the left uterine horn 9 weeks after PDT with topical applied ALA (58 mg/kg in .15 ml sterile H_2O intrauterine) and 80 J/cm^2. The endometrium has been destroyed by PDT, whereas the longitudinal and circular myometrial layers remained intact.

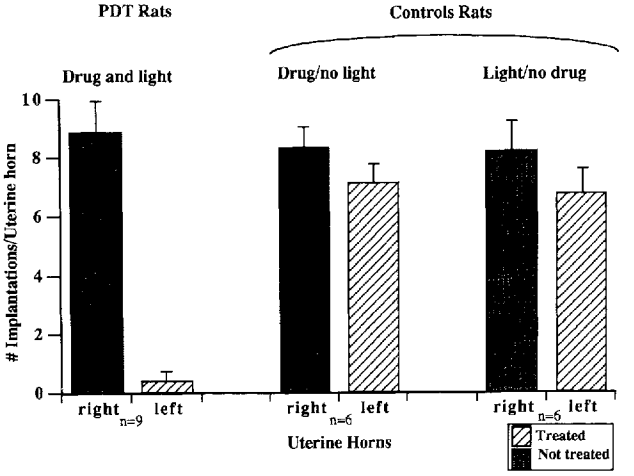

Fig. 5. Reproductive performance after PDT with ALA (58 mg/kg in .15 ml sterile H_2O intrauterine) and laser light (630 nm, 80 J/cm^2). Differences between implantations/rat (means with standard error) in the treated area of the left uterine horn and in the right horn are significant only for the study group ($P < 0.01$).

during the next 2–3 weeks. The arteries appeared as if returned to normal, whereas the tunica muscularis still seemed to be somewhat "disorganized." The lamina propria appeared less cellular, with an increased amount of collagen. Interestingly, cells in the zona compacta were less responsive to cyclic changes than the untreated control uterine horns. Although signs of regeneration were visible, treated areas typically showed marked endometrial atrophy, even following exposure to estrogen stimulation that resulted from pregnancy in the contralateral (nontreated) uterine horn 7–10 weeks after PDT (Fig. 4). There were no macroscopic or microscopic changes in the control uterine horns, neither in the tissue exposed to illumination without priming nor to the sensitizer alone.

Reproductive performance. There was a significantly lower number of gestational sacs in the PDT area of the left uterine horns (0.4 ± 0.3) as compared with the corresponding area of the untreated side (8.9 ± 1.0, $P < 0.01$) (Fig. 5). Control animals (light without drug and drug without light) exhibited no significant difference in the number of implantations (8.2 ± 1.0 vs. 6.8 ± 0.9 and 8.3 ± 0.7 vs. 7.2 ± 0.6, respectively). Figure 6 illustrates a pregnant uterus excised from an animal mated 3 weeks following PDT. The nontreated horn contained multiple gestational sacs, whereas no implantations occurred in the treated horn.

Thermal measurements during PDT. Illumination of uteri with 80 J/cm^2 induced a temperature rise of 6.5°C, which was noted within 2 minutes and leveled off thereafter. Switching off the light source was followed by an equally rapid temperature drop to the pretreatment level. The highest recorded temperature was 31.9°C in one rat and 33.6°C in the other. Moistening the tissue with saline during treatment resulted in a significant cooling of the treated area for a period of 2–3 minutes.

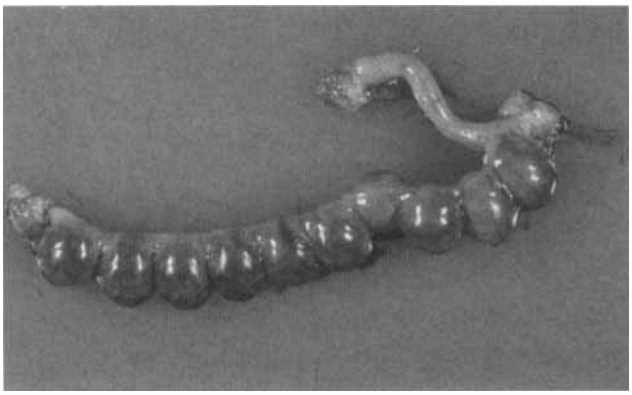

Fig. 6. Excised uterus 8 weeks after PDT with intrauterine application of ALA (58 mg/kg in .15 ml sterile H_2O intrauterine) and 80 J/cm^2. The functional integrity of the right uterine horn is demonstrated by 10 intact implantations, whereas there are no gestational sacs in the PDT-treated left uterine horn.

DISCUSSION

A minimally invasive approach for endometrial ablation may have a significant impact on

the treatment of dysfunctional uterine bleeding and on indications for hysterectomy. Several aspects of the conversion of ALA in rat uteri to the potent photosensitizer PpIX, and the efficacy of PDT for selective endometrial destruction were studied.

Topical application of a photosensitizer for endometrial targeting may eliminate skin photosensitivity, which is the main side effect of PDT following systemic application of porphyrin derivatives [12–14]. Skin photosensitivity was tested in the reproductive performance section of our study, and none of the animals showed any alterations in the light-treated skin area.

Fluorescence microscopy studies revealed comparable fluorescence levels in the endometrial stroma and myometrium 3–6 hours following intrauterine administration of ALA (Fig. 1). Interestingly, drug uptake and conversion, as demonstrated by digital fluorescence microscopy, showed a significantly higher concentration in the endometrial glands (Figs. 1 and 2). This observation provides the background for selective targeting of structures within the endometrium. The pharmacokinetic curve suggests that the optimal window for illumination-induced PDT is at 3–6 hours.

It is known that ALA-Pp IX conversion in the heme biosynthetic pathway occurs in the mitochondria. The computer-generated fluorescent images suggested that Pp IX is accumulated in the cytoplasm and around the membrane, and may be the source of the multilocular and complex destructive mechanism (Fig. 3).

Histological studies revealed clear signs of destruction throughout the endometrial layer after PDT, and in some specimens even the myometrial layers showed distinct areas of necrosis. This finding is consistent with our observation on drug distribution in the myometrium (Figs. 1 and 2b), and contrasts with the work of others [19], who described a selective destruction of the endometrium in the rat using the same drug but a different light source and delivery. The inconsistency in the tissue destruction pattern may be related to the nonhomogenous light distribution of the diffusing fiber tip, as was documented in the sensitive thermographic imaging. The lack of damage in the control uteri and the minimal thermal fluctuations under the threshold of potential effects documented in this study are indicative of photochemical changes.

The observation of a visible endometrial effect following PDT was also confirmed by functional assay. The reproductive performance study demonstrated a significant implantation failure in the treated uterine horns as compared with various controls. Noteworthy, the pregnancy rate was assessed at 3–4 weeks following PDT, a phase at which in some animals endometrial regeneration was demonstrated histologically. This is suggestive of nonvisible functional damage. It is not clear if similar protocols in the human will cause similar effects; however, systematic PDT studies were designed to explore the mechanisms of endometrial regeneration and proliferation.

Myometrial damage observed in our study may not limit the conversion of this technology to the human, since the combination of myometrial thickness and limited light penetration will protect undesired deep damage. Information on the optical properties of the human uterus and propagation of light through the endometrium and myometrium is currently being tested in order to design protocols for endometrial PDT. Indications for such minimally invasive treatment might be dysfunctional uterine bleeding endometriosis, adenomyosis, and permanent sterilization.

ACKNOWLEDGMENTS

This research was supported by grants Krebsliga des Kantons, Zürich, Switzerland and NIH 2RO1 CA32248 and 5P41 RR01192, DOE DE-FG03-91ER61227, and ONR N00014-91-C-0134 to Memorial Health Services.

REFERENCES

1. Raab C. Über die Wirkung fluoreszierender Stoffe auf Infusoria (abstract). Z Biol 1990; 39:524.
2. Dougherty TJ, Grindey GB, Fiel R, Weishaupt KR, Boyle DG. Photoradiation treatment II. Cure of animal tumors with hematoporphyrins and light. J Natl Cancer Inst 1975; 55:115–121.
3. Kimel S, Tromberg BJ, Roberts WG, Berns WM. Singlet oxygen generation of porphyrins, chlorins and phthalocyanines. Photochem Photobiol 1989; 50:175–183.
4. Berns MW, Dahlman A, Johnson FM, Burns R, Sperling D, Guiltiman D, Siemens A, Walter R. Wright W, Hammer-Wilson M, Wile A. A in vitro cellular effects of hematoporphyrin derivative. Cancer Res 1982; 42:2325–2329.
5. Modica-Napolitano JS, Joyal JL, Ara G, Oseroff AR, Aprille JR. Mitochondrial toxicity of cationic photosensitizers for photochemotherapy. Cancer Res 1990; 50:7876–7881.
6. Singh GP, Jeeves P, Wilson BC, Jang D. Mitochondrial photosensitization by Photophrin II. Photochem Photobiol 1987; 46:645–649.

7. Chaudhuri K, Keck RW, Selman SH. Morphological changes of tumor microvasculare following hematoporphyrin derivative sensitized photodynamic therapy. Photochem Photobiol 1987; 46:823–827.
8. Nelson JS, Liaw LH, Orenstein A, Roberts WG, Berns MW. Mechanism of tumor destruction following photodynamic therapy with hematoporphyrin derivative, chlorin, and phtalocyanine. J Natl Cancer Inst 1988; 80:1599–1605.
9. Star WM, Marijnissen HPA, van den Berg-Block, AE, Versteeg JAC, Franken KAP, Reinhold HS. Destruction of rat mammary tumor and normal tissue microcirculation by hematoporphyrin derivative photoradiation observed in vivo sandwich observation chambers. Cancer Res 1986; 46:2532–2540.
10. Manyak MJ, Nelson LM, DS, DeGraff W, Stillman RJ, Russo A. Photodynamic therapy of rabbit endometrial transplants: A model for treatment of endometriosis. Fertil Steril 1989; 52:140–144.
11. Schneider DF, Schellhas HF, Wesseler TA, Moulton BC. Endometrial ablation by DHE photoradiation therapy in estrogen-treated ovariectomized rats. Colposcopy Gynecol Laser Surg 1988; 4:73–85.
12. Dougherty TJ, Cooper MT, Mang TS. Cuteanous phototoxic occurrences in patients receiving photofrin. Lasers Surg Med 1990; 10:185–188.
13. Razum N, Balchum OJ, Profio AE, Carstens F. Skin photosensitivity: Duration and intensity following intravenous hematoporphyrin derivatives HpD and DHE. Photochem Photobiol 1987; 46:925–928.
14. Roberts WG, Smith KM, McCullough JL, Berns MW. Skin photosensitivity and photodestruction of several potentional photodynamic sensitizers. Photochem Photobiol 1989; 49:431–438.
15. Chapman JA, Tadir Y, Tromberg BJ, Yu K, Manetta A, Sun CH, Berns MW. Effect of administration route and estrogen manipulation on endometrial uptake of Photofrin porfimer sodium. Am J Obstet Gynecol 1993; 168: 685–692.
16. Kennedy JC, Pottier RH, Pross DC. Photodynamic therapy with endogenous protoporphyrin IX: Basic principles and present clinical experience. J Photochem Photobiol B 1990; 6:143–148.
17. Kennedy JC, Pottier RH. Endogenous protoporphyrin IX, a clinically useful photosensitizer for photodynamic therapy. J Photochem Photobiol B 1992; 14:275–292.
18. Yuan YD. Female reproductive system. In: Haschel W, ed. "Handbook of Toxicologic Pathology." San Diego: Academic Press, 1991, pp 891–935.
19. Yang JZ, Van Vught DA, Kennedy JC, Reid RL. Evidence of lasting functional destruction of the rat endometrium after 5-aminolevulinic acid induced photodynamic ablation: Prevention of implantation. Am J Obstet Gynecol 1993; 168:995–1000.